EVALUATING STRATEGIES FOR GROUND TRACK ACQUISITION AND ORBITAL PHASING

Sérgio Brás[1], Itziar Barat[2], and Berthyl Duesmann[3]

[1] *Portuguese Trainee @ ESA/ESTEC, keplerlaan 1 2200AG NL, Sergio.Bras@esa.int*

[2] *Deimos-Space @ ESA/ESTEC, keplerlaan 1 2200AG NL, Itziar.Barat@esa.int*

[3] *ESA/ESTEC, keplerlaan 1 2200AG NL, Berthyl.Duesmann@esa.int*

Abstract: *This paper addresses the problem of the design and analysis of suitable manoeuvring strategies for ground track acquisition and orbital phasing. Often, the nominal altitude should be achieved as soon as possible to allow instrument calibration and other commissioning activities. We propose a constructive approach based on a perturbation analysis of the nominal orbit. With the help of an in-house tool, a parametric study which considers the launch dispersions and the a priori unknown initial phase is performed to assess the expected duration and Delta-V consumption to reach the desired orbit from the satellite's injection orbit. Different algorithms are available that either minimise the duration of the orbit acquisition phase or minimise the required Delta-V. Several constrains are considered, such as, available Delta-V, propulsion performance, and operational restrictions, namely number orbit corrections performed per day, maximum Delta-V achieved per manoeuvre, and non-available days for manoeuvring. Additionally, calibration and tuning manoeuvres are taken into account. A general overview of the different factors affecting the orbit acquisition will be given followed by some examples, namely, Sentinel-1B, Sentinel 2-B, and Sentinel-5P.*

Keywords: *Orbit acquisition, phasing, repeat ground track*

1. Introduction

Repeat ground track orbits are of paramount importance for Earth observation missions as they allow the acquisition of the same scene at fixed time intervals. Either for calibration or nominal operation proposes, many satellites are required to overpass an exact location on Earth. Additionally, for missions comprising spacecraft constellations, accurate orbit phasing is also needed. The satellite manoeuvres should be carefully planned to control the ground track drift so that the desired longitude at ascending node crossing (ANX) are achieved. Moreover, the duration of the orbit acquisition phase depends on constraints such as the number of manoeuvres per week, thrusters characteristics, and Delta-V budget.

The work in [1] describes an analytical methodology for modelling the ground track drift of a low-Earth satellite as well as the semi-major axis and eccentricity change for a given impulsive in-plane Delta-V. The modelling is based on linearization of ground track shift from one pass to the next. Then the developed analytical formulation is implemented computationally and used to select the manoeuvres of the orbit acquisition process.

The conditions required for repeat ground track orbits are analysed in [2]. In this work, an autonomous orbit control system to drive the satellite from any initial condition to the desired repeat ground track is also outlined. Similarly to [1], the control concept is based on the linearized model of the nodal period.

The works in [1] and [2] provide a theoretical framework for the analysis and design of a orbit acquisition phase. However, constraints that limit the manoeuvring strategies and that are inherently present on any mission are not addressed. The different scenarios analysed for the orbit acquisition of MetOp-A are described in [3] as well as the actual manoeuvre executed to achieve the desired orbit position. The ground track was required to be achieved within two weeks. During the Launch and Early Orbit Phase (LEOP) there were two opportunities for performing orbital corrections on the third and last day. Since the out-of-plane manoeuvres have an in-plane component and vice-versa, the last manoeuvre had to be a small in-plane manoeuvre to correct eventual inaccuracies and cross component effects of previous manoeuvres. Some orbit acquisition strategies were studied before launch to prepare the LEOP. Four cases were considered: i) the initial semi-major axis yields a ground track drift such that only a drift stop manoeuvre is required in less than two weeks; ii) an in-plane manoeuvre is necessary to adjust the initial ground track drift towards the closest orbital node; iii) an in-plane manoeuvre is necessary to adjust the initial ground track drift towards a different orbital node; iv) no attempt to achieve the desired ground track is performed and only the semi-major axis, eccentricity, and inclination are corrected to their nominal values. After launch, during LEOP, two options were considered: i) to reverse the drift to the closest node, which has a smaller manoeuvre size, and ii) to slow down the drift to the next node, which would consume less propellant. In the end, the former was considered.

The description of the orbit acquisition manoeuvres of MetOp-B as well as the associate preliminary studies are presented in [4] and [5]. The ground track of MetOp-B is the same as MetOp-A, and is was decided to phase its orbit such that the revisit time was 12 or 17 days, which corresponds to an orbital angular difference of 173.793 deg [5]. Similarly to MetOp-A, only two opportunities for correcting the initial orbit were available on the third day of LEOP. This orbit acquisition scenario had higher complexity that the one of MetOp-A, since only two nodes would lead to the proper phasing between both satellites. The fact that the initial phasing of the two satellites depends on the launch day adds additional challenges to the analysis. The first manoeuvre had to be conservative since the thrusters preformed were not yet calibrated. The last manoeuvre should also be small to minimise the consequences of thrust uncertainties and to guarantee that the desired ground track is achieved. The selection of the orbit acquisition strategy had to take into account the available times for manoeuvring had to minimise the propellant consumption, phase duration, and interference with MetOp-A. Instrument decontamination constraints and the time required to determine the orbit and to prepare a new manoeuvre lead to only two manoeuvring opportunities on the third day and that a drift stop manoeuvre was not possible before the day 5 after LEOP. Thus, the objective was to achieve the desired ground track within 5 to 14 days after the end of LEOP and avoid interferences with MetOp-A if possible.

As illustrated by the cases of MetOp-A and MetOp-B, mission constraints and parameters of the injection orbit have significant impact on the characteristics of the orbit acquisition phase, namely on its duration and propellant consumption. However, often only a few acquisition scenarios are studied prior to launch. To address this issue an in-house tool was developed that automatically computes the set of manoeuvres required to acquire the proper ground track and orbital phasing while minimizing either the duration or the Delta-V consumption. The tool can be used to perform a parametric analysis of the impact of the mission parameters, such as, day of launch, semi-major axis dispersion, and manoeuvring capabilities. Another application of this tool is the computation of a preliminary orbit acquisition scenario once the launch orbit is known. In some missions, the nominal orbit needs to be acquired as soon as possible and the orbit corrections need to be initiated before the end of LEOP. Usually, optimization tools take long to analyse each case and initial conditions are required. This tool can be used to speed up this process by performing a holistic assessment of several strategies before using a full force model software.

This paper addresses the criteria for selecting the injection orbit and the ground track acquisition strategies. A perturbation analysis of the ground track drift with respect to semi-major axis is presented. The impact of different mission constraints to the acquisition strategy is described. Moreover, some representative acquisition examples are given.

This remaining of this paper is organized as follows. In Section 2 a brief introduction to Sun-synchronous orbits is presented. A perturbation analysis of the ground track drift with respect to the semi-major axis and inclination is given in Section 3. The several mission characteristics that constraint the orbit acquisition strategies are described in Section 4 and their impact is assessed in Section 5. Section 6 illustrates the analysis in Section 5, by providing examples of orbit acquisition scenarios of several Earth observation missions.

2. Sun-synchronous orbits

Earth observation satellites are specially designed for environmental monitoring and mapping of our planet. Since the accuracy and sensitivity of the remote sensing instruments degrades with the altitude, most Earth observation satellites are operated in a low-Earth orbit (LEO), i.e. at altitudes approximately between 200 km and 2000 km. Sun-synchronous orbits are near circular with altitudes, mostly, between 600 km and 800 km. In these orbits, the orientation of the orbital plane with respect to the Sun is approximately constant and the satellite observes a scene on ground always with the same illumination conditions. This has several advantages for Earth observation. For passive imaging satellites which rely on the light reflected by the Earth, with Sun incidence angle different from 90 deg are advantageous to reduce Sun glint. On the other hand, radar satellites can be placed on dawn/dusk orbits, so that they receive solar power during mostly of of the time which maximizes the active time of the instruments.

The Mean Local Solar Time (MLST) is used to characterize the Sun lightning conditions. The MLST of an equator crossing (ascending or descending node) at longitude L (expressed in degrees) is given by [6]

$$\mathbf{MLST} \cong \mathbf{UT} + \mathbf{L}\frac{\mathbf{24}}{\mathbf{360}}(\mathbf{hours}), \tag{1}$$

where UT is the universal time based on the Earth's rotation expressed in hours. Consequently, UT is the MLST at 0 deg longitude. This time is constant in Sun-synchronous orbits. The constant orientation of the orbit plane with respect to the direction of the Sun is achieved by a judicious selection of the orbital parameters, in particular, of semi-major axis, eccentricity, and inclination, so that the perturbation effect due to the Earth oblateness results in a rotation of the right ascension of the ascending node Ω (angle from the vernal equinox to the ascending node). The Earth makes a full translation around the Sun in 365.2421897 days [7]. Hence, the motion of a Sun-synchronous orbit is characterized by

$$\dot{\boldsymbol{\Omega}} = \dot{\boldsymbol{\Omega}}_{ss} = \frac{\mathbf{360}}{\mathbf{365.2421897}}\,\mathbf{deg/day}. \tag{2}$$

The dominant motion of Ω is caused by J_2, which represents Earth's oblateness and it is described by

$$\dot{\boldsymbol{\Omega}}_{J_2} = -\frac{3}{2}\sqrt{\frac{\mu}{a^7}}\frac{R_\oplus}{(1-e^2)^2}\cos(\boldsymbol{i}), \tag{3}$$

where μ denotes the gravitational constant, $\boldsymbol{R}_\oplus$ is the Earth's radius, a is the semi-major axis of the satellite's orbit, e is the orbit eccentricity, and i is the orbit inclination.

Sun-synchronous orbits can be designed such that the satellite has a specific repeat ground track, i.e. it passes over the exact same location on the earth surface at fixed time intervals. This is important to guarantee passes over ground stations and for monitoring the evolution of terrain over time (e.g. shoreline, land-coverage, and land-change). The nodal period of an orbit is approximately given by [7]

$$\boldsymbol{P}_{\boldsymbol{\Omega}} = 2\boldsymbol{\pi}\sqrt{\frac{a^3}{\mu}}\left(\mathbf{1} + \frac{3J_2R_\oplus^2}{2a^2}(\mathbf{3} - \mathbf{4}\sin^2(\boldsymbol{i})\right). \tag{4}$$

The nodal period of repeat ground track orbits composed of k_{rev} revolutions repeated after k_{days} days satisfies

$$\boldsymbol{P}_{\boldsymbol{\Omega}}(\boldsymbol{\omega}_\oplus - \dot{\boldsymbol{\Omega}}) = \frac{k_{days}}{k_{rev}}, \tag{5}$$

where $\omega_\oplus$ denotes the Earth rotation velocity.

3. Ground track acquisition based on perturbation analysis of the nominal orbit

After the launch, the orbit of the satellite needs to be adjusted to the targeted a, i, and e and, if it is the case, to the desired ground track. If the target Sun-synchronous orbit does not have a specific ground track or phasing with respect to other satellite, the orbit is achieved simply by applying manoeuvre corrections to the initial injection orbit so that a, i, and e become nominal. However, if the satellite has a targeted ground track or needs to be phased with other satellite, the manoeuvring plan should take that into account.

The ground track is achieved by reducing or increasing the orbital period so that the ascending node drifts to the East or to the West, respectively. From Eq. 4, we have that the nodal period depends considerably on the semi-major axis, a. Thus, by performing in-plane manoeuvres, the semi-major axis can be controlled to achieve the desired ground track. For the same propellant, inclination changes have a much smaller effect on the nodal period. Nevertheless, inclination also needs to be taken into account in the design orbit acquisition phase. We resort to a perturbation analysis of the nominal orbit to study the consequences to the ground track acquisition of small variations on a and i. In this analysis, only the J_2 zonal harmonic of Earth's gravity field is considered (since this is a first order perturbation analysis). The mathematical derivation follows mostly the work in [7].

The equatorial distance between two consecutive (in time) nodes is given by

$$\boldsymbol{\lambda}_{one\,rev} = \mathbf{R}_\oplus(\boldsymbol{\omega}_\oplus - \dot{\boldsymbol{\Omega}})\mathbf{P}_{\boldsymbol{\Omega}}. \tag{6}$$

On the other hand, by the definition of Sun-synchronous orbit, we have that

$$\boldsymbol{\lambda_{one\,rev}} = \frac{\mathbf{2\pi R_{\oplus}} \boldsymbol{k_{days}}}{\boldsymbol{k_{rev}}}. \tag{7}$$

Let us define a reference orbit characterized by nominal a, i, and e, and in which $\lambda_{ref}\ (t_{ref})$ is the equatorial position of the ascending node at instant t_{ref} . The mean time evolution of λ_{ref} is given by

$$\boldsymbol{\lambda_{ref}(t)} = \mathbf{mod}\big(\mathrm{R}_{\oplus}(\boldsymbol{\omega_{\oplus}} - \dot{\boldsymbol{\Omega}}_{SS})(\boldsymbol{t_0} - \boldsymbol{t_{ref}}) + \boldsymbol{\lambda_{ref}}(\boldsymbol{t_{ref}}), \mathbf{2}\boldsymbol{\pi R_{\oplus}}\big), \tag{8}$$

$$= \mathbf{mod}\left(\frac{\mathrm{R}_{\oplus}(\omega_{\oplus} - \dot{\Omega})}{P_{\Omega}}\,\frac{k_{days}}{k_{rev}}(\boldsymbol{t} - \boldsymbol{t_{ref}}) + \boldsymbol{\lambda_{ref}}(\boldsymbol{t_{ref}}), \mathbf{2}\boldsymbol{\pi R_{\oplus}}\right). \tag{9}$$

where $\mathrm{mod}(a, b)$ denotes the modulo operation, i.e. the remainder after division of a by b. From the initial estimation of the injection orbit, we compute the equatorial position of the first ascending node λ_0 at time t_0. Then, the equatorial distance of the first ascending node to the one of the reference orbit is

$$\boldsymbol{\Delta\lambda_0} = \boldsymbol{\lambda_0} - \boldsymbol{\lambda_{ref}}(\boldsymbol{t_0}) \tag{10}$$

$$= \boldsymbol{\lambda_0} - \mathbf{mod}\left(\frac{\mathrm{R}_{\oplus}(\omega_{\oplus} - \dot{\Omega})}{P_{\Omega}}\,\frac{k_{days}}{k_{rev}}(\boldsymbol{t_0} - \boldsymbol{t_{ref}}) + \boldsymbol{\lambda_{ref}}(\boldsymbol{t_{ref}}), \mathbf{2}\boldsymbol{\pi R_{\oplus}}\right). \tag{11}$$

Notice that $|\boldsymbol{\Delta\lambda_0}| \leq 2\pi R_{\oplus} \frac{k_{day}}{k_{rev}}$, otherwise the initial ascending node would not have the same MSLT of the reference orbit. For sake of simplicity, define

$$\boldsymbol{\Delta\lambda_0^+} = \boldsymbol{mod}\left(\boldsymbol{\Delta\lambda_0}, \mathbf{2}\boldsymbol{\pi R_{\oplus}}\frac{\boldsymbol{k_{days}}}{\boldsymbol{k_{rev}}}\right), \tag{12}$$

so that it is guaranteed that $\boldsymbol{\Delta\lambda_0^+}$ has a positive value.

Assuming small variations of a and i (e is assumed to be nominal, and thus not included in this analysis), Eq. 6 can be approximated by

$$\boldsymbol{\lambda_{one\,rev}}(\boldsymbol{a} + \boldsymbol{\Delta a}, \boldsymbol{i} + \boldsymbol{\Delta i}) \approx \boldsymbol{\lambda_{one\,rev}}(\boldsymbol{a}, \boldsymbol{i}) + \frac{\partial \boldsymbol{\lambda_{one\,rev}}\,(\boldsymbol{a},\boldsymbol{i})}{\partial \boldsymbol{a}}\boldsymbol{\Delta a} + \frac{\partial \boldsymbol{\lambda_{one\,rev}}\,(\boldsymbol{a},\boldsymbol{i})}{\partial \boldsymbol{i}}\boldsymbol{\Delta i}. \tag{13}$$

The partial derivative of $\lambda_{one\,rev}$ with respect to a is given by

$$\frac{\partial \boldsymbol{\lambda_{one\,rev}}\,(\boldsymbol{a},\boldsymbol{i})}{\partial \boldsymbol{a}} = \boldsymbol{R_{\oplus}}(\boldsymbol{\omega_{\oplus}} - \dot{\boldsymbol{\Omega}})\frac{\partial \boldsymbol{P_{\Omega}}}{\partial \boldsymbol{a}} - \boldsymbol{R_{\oplus}}\boldsymbol{P_{\Omega}}\frac{\partial \dot{\boldsymbol{\Omega}}}{\partial \boldsymbol{a}}. \tag{14}$$

where the partial derivative of Eq. 4 yields

$$\frac{\partial P_\Omega}{\partial a} \approx \frac{21}{4}\sqrt{\frac{\mu}{a^9}}\frac{R_\oplus^2 J_2}{\left(1-e^2\right)^2}\cos(i), \tag{15}$$

and, ignoring high order zonal harmonics, by using Eq. 3, we obtain

$$\frac{\partial \dot{\Omega}}{\partial a} \approx 3\pi\sqrt{\frac{\mu}{a}}\left(1+\frac{J_2}{2}\left(\frac{R_\oplus^2}{a}\right)^2(3-4\sin^2(i))\right). \tag{16}$$

The partial derivative of $\lambda_{one\ rev}$ with respect to i is given by

$$\frac{\partial \lambda_{one\ rev}(a,i)}{\partial i} = R_\oplus(\omega_\oplus-\dot{\Omega})\frac{\partial P_\Omega}{\partial i} - R_\oplus P_\Omega\frac{\partial \dot{\Omega}}{\partial i}. \tag{17}$$

where the partial derivative of Eq. 4 yields

$$\frac{\partial P_\Omega}{\partial i} \approx -12\pi\sqrt{\frac{a^7}{\mu}}R_\oplus^2\sin(2i), \tag{18}$$

and, neglecting high order zonal harmonics, by using Eq. 3, we obtain

$$\frac{\partial \dot{\Omega}}{\partial i} \approx \frac{3}{2}\sqrt{\frac{\mu}{a^7}}\frac{R_\oplus^2 J_2}{\left(1-e^2\right)^2}\sin(i). \tag{19}$$

Expressing continuously in time the difference between the nominal and the perturbed orbits, we obtain

$$\Delta\lambda(t) = \int_{t_0}^{t}\frac{\lambda_{one\ rev}(a+\Delta a, i+\Delta i)-\lambda_{one\ rev}(a,i)}{P_\Omega}dt \tag{20}$$

$$= \frac{1}{P_\Omega}\int_{t_0}^{t}\left(\frac{\partial \lambda_{one\ rev}(a,i)}{\partial a}\Delta a + \frac{\partial \lambda_{one\ rev}(a,i)}{\partial i}\Delta i\right)dt \tag{21}$$

$$= \frac{1}{P_\Omega}\left(\frac{\partial \lambda_{one\ rev}(a,i)}{\partial a}\int_{t_0}^{t}\Delta a(t)\,dt + \frac{\partial \lambda_{one\ rev}(a,i)}{\partial i}\int_{t_0}^{t}\Delta i(t)\,dt\right). \tag{22}$$

The orbital nodes of a orbit with 10 days repeat cycle are depicted in Fig. 1. Notice that the ground track ascending nodes have a analogue in the orbital plane representation. In this example, the satellite is launched between nodes 4 and 5. In case the satellite is to be placed in node 1, $\Delta a(t)$ and $\Delta i(t)$ should be controlled so that at t_{end}, we have

$$\Delta\lambda(t_{end}) = k\lambda_{one\ rev} - \Delta\lambda_0^+, k \in \mathbb{Z}. \tag{23}$$

On the other hand, the desired ground track is achieved in any of the nodes. In this case, the ground track is achieved at time t_{end} if

$$\Delta\lambda(t_{end}) = k\frac{\lambda_{one\ rev}}{k_{days}} - \Delta\lambda_0^+, k \in \mathbb{Z}. \tag{24}$$

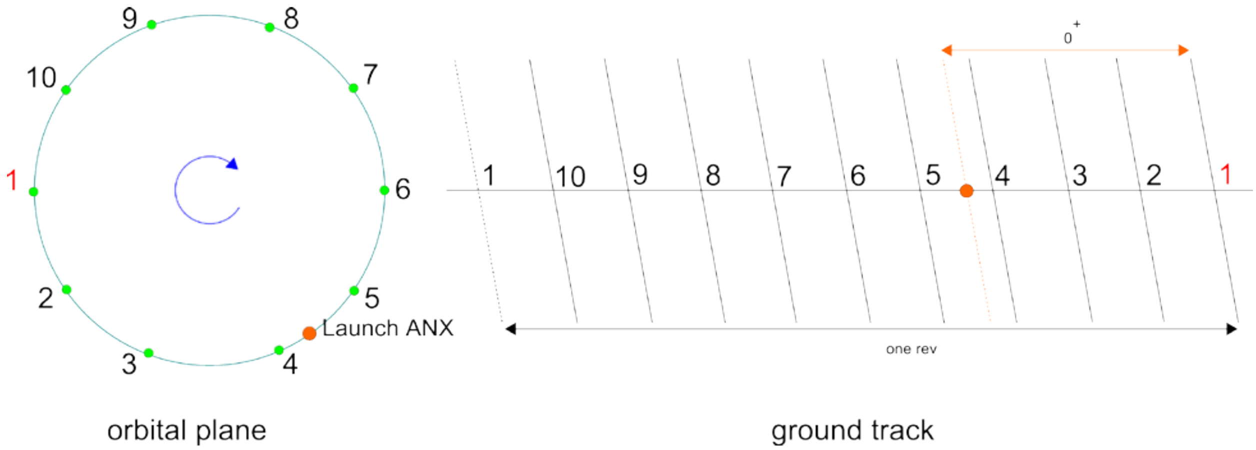

Figure 1. Representation of the orbital nodes on the orbital plane and on the ground track

In general, changing the $\Delta a(t)$ is more efficient than modifying $\Delta i(t)$. For this reason, for sake of simplicity, let us assume that $\Delta i(t) = 0$. Hence,

$$\Delta\lambda_{\Delta i(t)=0}(t) = \frac{1}{P_\Omega}\frac{\partial \lambda_{one\,rev}(a,i)}{\partial a}\int_{t_0}^{t}\Delta a(t)\,dt. \tag{25}$$

From Eq. 25, we conclude that the ground track drift is closely associated with the area given by the integration of the semi-major axis time evolution, i.e. with $A = \int_{t_0}^{t}\Delta a(t)\,dt$. Given the typical duration of the in-plane manoeuvres, one can further simplify Eq. 25 by assuming that semi-major axis changes occur instantaneously in time. An example of $\Delta a(t)$ evolution is shown in Fig. 2.

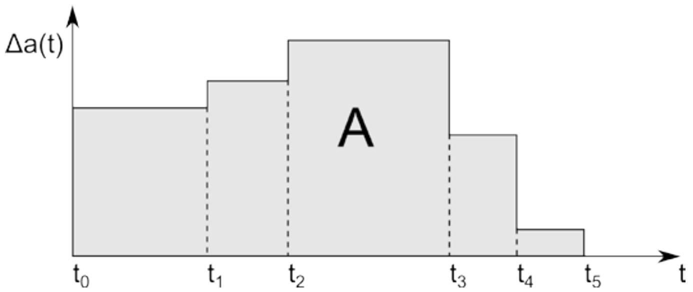

Figure 2. Semi-major axis time evolution (assuming impulsive manoeuvres)

Thus, the problem of ground track acquisition can be posed as optimal the selection of the orbital manoeuvres that guarantee

$$A = \int_{t_0}^{t_{end}}\Delta a(t)\,dt \tag{26}$$

$$= P_\Omega\left(\frac{\partial \lambda_{one\,rev}(a,i)}{\partial a}\right)^{-1}\left(k\frac{\lambda_{one\,rev}}{k_{days}} - \Delta\lambda_0^{+}\right), k \in \mathbb{Z}, \tag{27}$$

while minimizing the acquisition time t_{end}. The optimal selection of the in-plane manoeuvres is subject to several constraints: operational, planning, platform limits, and instrument safety. For instance, it is usual to have a period without manoeuvres after launch, and the first and last manoeuvres are normally smaller than the others, to allow thruster calibration and to minimize effects of thruster misperformance, respectively. However, these constraints vary from mission to mission. Thus, a systematic analysis of the impact of different design options calls for automatic algorithms that produce suitable orbit acquisition solutions while taking into account the mission constraints.

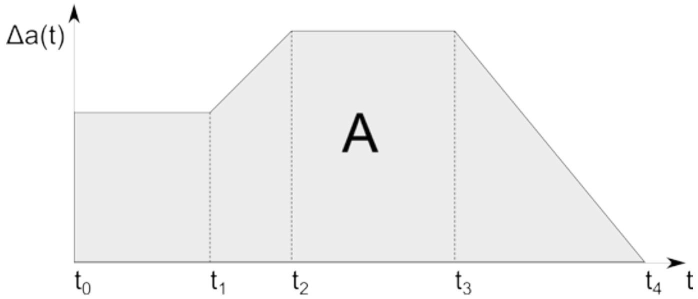

Figure 3. Semi-major axis time evolution (assuming continuous semi-major axis change rate)

If the orbit acquisition phase has a long duration, due to the mission requirements or due to the eventual on-board low thrust capabilities, the analysis can be further simplified by assuming a constant rate of change of the semi-major axis. This case is illustrated in Fig. 3.

4. Mission constraints

The design of a ground track acquisition phase needs to satisfy the mission constraints, which can be categorized in different groups:

- Platform constraints: Delta-V budget, maximum Delta-V per manoeuvre, realization of a small calibration manoeuvre, the last manoeuvre should also be conservative to minimize the effects of eventual burn misperformance, eventual yaw manoeuvres should not jeopardise thermal control.
- Operational constraints: maximum manoeuvring frequency (due to orbit determination and planning), manoeuvring during visibility, preferred time-windows for the orbital corrections.
- Planning constraints: other scheduled LEOP activities.
- Instrument constraints: some instruments cannot be orientated towards the Sun, thus, manoeuvres that involve rotations may need to be performed during eclipse.

Exploiting Eq. 22, algorithms were developed that compute the manoeuvring instants and the corresponding magnitudes that minimize either the duration of the orbit acquisition phase or the Delta-V consumption. These algorithms are implemented in an in-house tool that take into account the mission constraints. In particular, it is possible to set the initial semi-major axis difference with respect to the nominal, the launch date, the targeted orbital node (if required), the period of time after launch during which manoeuvres cannot be performed, the period of time between orbit corrections, the maximum and minimum magnitudes of the first manoeuvre, the maximum and minimum magnitudes of the last manoeuvre, the maximum magnitude of the intermediate manoeuvres, and the maximum Delta-V budget dedicated to the orbit acquisition phase. The tool can be used to compute the instants and magnitude of the orbit acquisition manoeuvres given a specific injection orbit. Moreover, it also allows to perform a parametric study of the impact of the semi-major axis dispersion and launch date as well as the mission constraints.

5. Assessment of the impact of the mission constraints on the orbit acquisition

As an illustrative example, let us consider a satellite to be launched to a Sun-synchronous orbit with the characteristics given in Tab. 1.

Table 1. Mean orbital characteristics

semi-major axis	7164267 m
eccentricity	0.001159
inclination	98.569 deg
reference longitude at ANX	0 deg
MLST	10h00
repeat cycle	10 days
cycle length	143 orbits

Moreover, assume that the mission constraints require a period of 5 days after launch without manoeuvres. The first orbital change should be a conservative calibration manoeuvre with Delta-V between 0.1 m/s and 0.3 m/s (either prograde or retrograde direction). To perform a soft touch-up, the last manoeuvre should also be small with Delta-V between 0.1 m/s and 0.3 m/s. The remaining manoeuvres can have maximum Delta-V of 1.5 m/s. Due to the orbit determination and planning times, one manoeuvre per day was possible. The launcher has a semi-major axis dispersion error of 10 km (3-sigma).

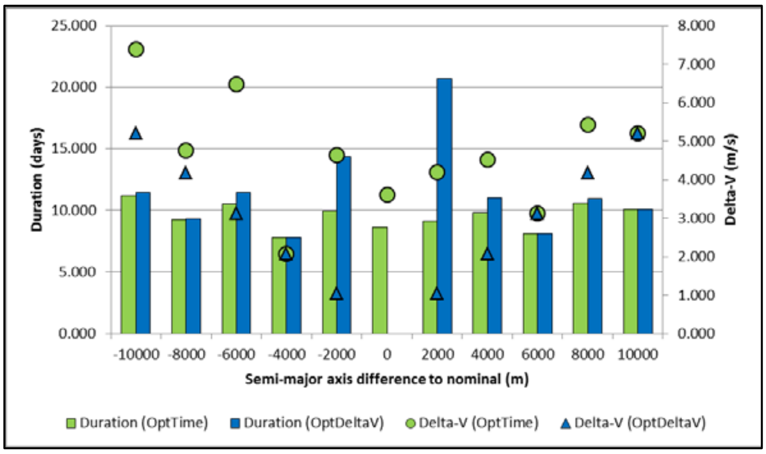

Figure 4. Orbit acquisition duration and Delta-V required for various semi-major axis differences to the nominal (Δsma).

Figure 4 shows the duration and the Delta-V required by the orbit acquisition strategy computed using the time minimising algorithm (OptTime) and the Delta-V minimising algorithm (OptDeltaV). The Delta-V minimising algorithm consists in making use of the natural drift induced by the initial semi-major axis. Therefore, when the satellite is launched exactly at the nominal semi-major axis, there is no natural drift and the algorithm does not produce a solution. It can be concluded that for some initial semi-major axis, the consumption of more propellant does not lead to significantly shorter acquisition times as in the cases of Δsma=−10000 m, Δsma=−6000 m, Δsma=−4000 m, and Δsma=8000 m. Moreover, for the analysed cases, it is possible to acquire the desired ground track in less than 11.5 days by using a maximum of 5.2 m/s Delta-V. For Δsma=2000 m, the possibility to increase the drift rate by an earlier manoeuvre allows a much shorter acquisition time than if only natural drift (drift induced by the initial Δsma) is used.

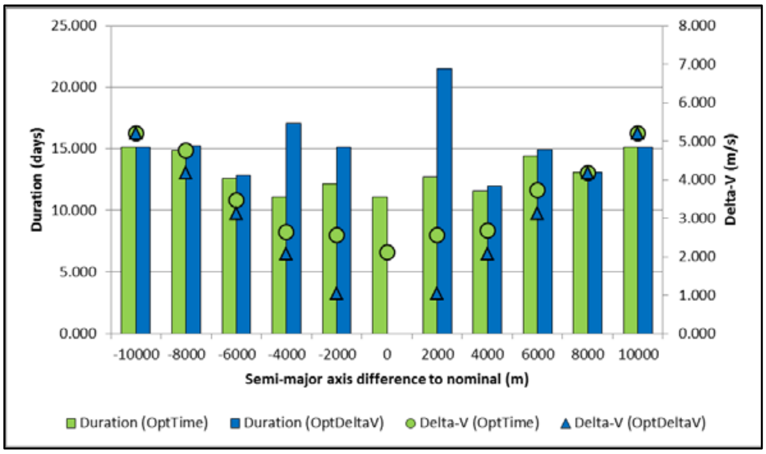

Figure 5. Orbit acquisition duration and Delta-V required for various semi-major axis differences to the nominal (Δsma) in case the time between manoeuvres is two days instead of one.

If the orbit determination and planning times take two days instead of one, the acquisition time is higher. This is illustrated in Fig. 5. In this case, the minimum acquisition time is around 11 days and can be up to 15 days for larger injection errors. Interesting enough, in this case, the minimisation of the duration of the orbit acquisition phase leads to smaller Delta-V consumption than in the previous case.

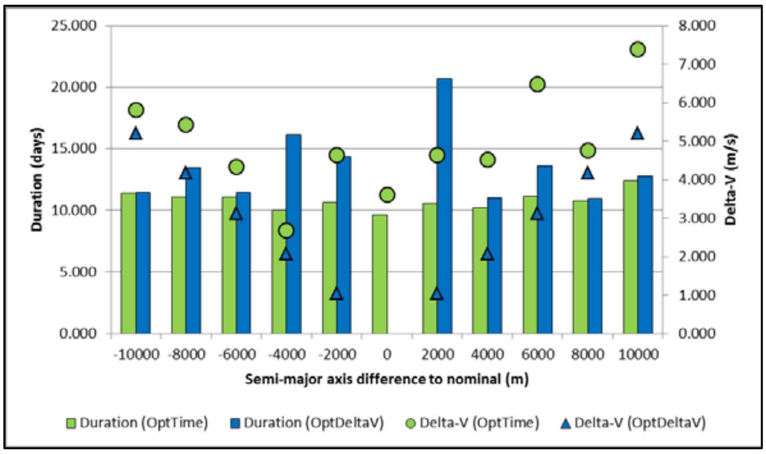

Figure 6. Orbit acquisition duration and Delta-V required for various semi-major axis differences to the nominal (Δsma) in case it is necessary to wait 6 days after launch before manoeuvres instead of 5 days.

Figure 6 depictes the case where the time window after launch without manoeuvres is 6 days instead of 5 days. For some initial dispersion errors, there is a significant increase of the duration of the orbit acquisition phase, namely for Δsma=−8000 m, Δsma=−4000 m, Δsma=6000 m, and Δsma=10000 m. This case highlights the advantage of correcting the initial orbit as early as possible.

6. Application to Copernicus program missions

Sentinel-1B, Sentinel 2-B and Sentinel-5P have significant different characteristics. Sentinel-1B and Sentinel-2B need to be phased approximately 180 deg with respect to their respective mission precursors. Sentinel-5P will fly in loose formation 5 minutes after Suomi-NPP.

Sentinel-2B is a standard case. It has a propulsion system with good performance and a comfortable Delta-V budget. Thus, performing extra manoeuvres to speed up the drift is not a major problem. Consequently, the altitude of the orbit targeted by the launcher is lower than the nominal altitude, which allows to increase the convergence to the desired final orbit position. It will be showed that, under reasonable launch dispersions and with small extra propellant consumption, the expected orbit acquisition duration remains within a month, depending mainly on the initial phasing with respect to Sentinel-2A rather than on the initial altitude difference.

Sentinel-1B might be an example of a satellite with a limited thrust propulsion system, where a minimum number of manoeuvres is preferred. For Sentinel-1B, the target altitude by the launcher is the nominal one, being the fact that the orbit is already occupied by Sentinel-1A a significant challenge. This has been addressed by imposing constraints on the initial phasing between both satellites in order to avoid collision and communication interference between both satellites again during LEOP.

In Sentinel-5P mission the available time to acquire the desired orbit and the Delta-V budget are not major constraints and the propulsion capability is ample. In this mission, safety is the driving factor both for the selected injection orbit and for the final approach to Suomi-NPP.

7. Conclusions

In this paper, a methodology for evaluating different strategies for ground track acquisition is described. Based on a perturbation analysis of the nominal orbit, a tool was developed that computes the manoeuvres that minimize either the duration of the acquisition phase or the Delta-V consumption while satisfying the mission constraints. This tool can be used to devise a preliminary acquisition strategy as well as to perform a parametric study of the impact of the mission constraints on the ground track acquisition duration and associated Delta-V budget. Several constrains were considered, such as, available Delta-V, propulsion performance, and operational restrictions, namely number orbit corrections performed per day, maximum Delta-V achieved per manoeuvre, and non-available days for manoeuvring. Additionally, calibration and tuning manoeuvres were also taken into account.

Future work will focus on improving the existent algorithms to allow the specification of the direction of the manoeuvres and also to automatically compute suitable inclination correction manoeuvres.

8. References

[1] Lee, B.-S., Eun, J.-W., and Webb, C. “Ground Track Acquisition and Maintenance Manoevre Modeling for Low-Earth Orbit Satellite.” Journal of Astronomy and Space Sciences, Vol. 14,pp. 355–366, 1997.

[2] Aorpimai, M. and Palmer, P. “Repeat-Groundtrack Orbit Acquisition and Maintenance for Earth-Observation Satellites.” Journal of Guidance, Control, and Dynamics, Vol. 30, pp. 654–659, 2007.

[3] K. Merz, K., Serrano, M., Kuijper, D., and Garc´ıa Matatoros, M. “The MetOp-A Orbit Acquisition Strategy and its LEOP Operational Experience.” Proceedings of the 20th International Symposium on Space Flight Dynamics – 20th ISSFD. Annapolis, MD, USA, 2007.

[4] Righetti, P., Sancho, F., and Paulino, T. “MetOp-B Orbit Acquisition Operations: Preparation and Execution.” Proceedings of the 23rd International Symposium on Space Flight Dynamics – 23rd ISSFD. Pasadena, CA, USA, 2012.

[5] Sánchez, J., Serrano, M., Kuijper, D., and Muñoz, I. “Design and Implementation of the MetOp-B Orbit Positioning Strategy.” Proceedings of the 23rd International Symposium on Space Flight Dynamics – 23rd ISSFD. Pasadena, CA, USA, 2012.

[6] Capderou, M. Handbook of Satellite Orbits. Springer, 2014.

[7] Vallado, D. and McClain,W. Fundamentals of Astrodynamics and Applications. Springer and Microcosm Press, 2007.